AMERICAN
METEOROLOGICAL
SOCIETY

Journal of Applied Meteorology and Climatology

The DOI for this manuscript is doi: 10.1175/JAMC-D-14-0320.1

The final published version of this manuscript will replace the preliminary version at the above DOI once it is available.

If you would like to cite this EOR in a separate work, please use the following full citation:

Booth, J., H. Rieder, D. Lee, and Y. Kushnir, 2015: The paths of extratropical cyclones associated with wintertime high wind events in the Northeast United States. J. Appl. Meteor. Climatol. doi:10.1175/JAMC-D-14-0320.1, in press.

The paths of extratropical cyclones associated with wintertime high wind events in the Northeast United States

James F Booth
Department of Earth and Atmospheric Sciences, City College of New York

Harald E Rieder
Wegener Center for Climate and Global Change and IGAM/Institute of Physics, University of Graz, Austria
Lamont Doherty Earth Observatory at Columbia University of New York

Dong Eun Lee and Yochanan Kushnir
Lamont Doherty Earth Observatory at Columbia University of New York

Corresponding Author: J. F. Booth, 160 Convent Avenue, Marshak Science Building Room 106, City College of New York, New York, NY 10031-9101 (jbooth@ccny.cuny.edu)

Abstract

This study analyzes the association between wintertime high wind events (HWEs) in the northeast United States and extratropical cyclones. Sustained wind maxima in the Daily Summary Data from the National Climatic Data Center's Integrated Surface Database are analyzed for 1979-2012. For each station, a Generalized Pareto Distribution (GPD) is fit to the upper tail of the daily maximum wind speed data, and probabilistic return levels at 1, 3 and 5-years are derived. Wind events meeting the return level criteria are termed HWEs. The HWEs occurring on the same day are grouped into simultaneous wind exceedance dates, termed multi-station events. In a separate analysis, extratropical cyclones are tracked using the ECMWF ERA-Interim reanalysis. The multi-station events are associated with the extratropical cyclone tracks based on cyclone proximity on the day of the event. The multi-station wind events are found to be most often associated with cyclones travelling from southwest to northeast, originating west of the Appalachian Mountains. To quantify the relative frequency of the strong wind associated cyclones, the full set of northeastern cyclone tracks are separated based on their path, using a crosshairs algorithm designed for this region. The tracks separate into an evenly distributed set of four pathways approaching the northeast US: from the due west, from the southwest, nor'easters, and storms starting off coast, north of the Carolinas. Using the frequency of the tracks in each of the pathways, it is shown that the storms associated with multi-station wind events are most likely to approach the northeast US from the southwest.

1. Introduction

A series of recent, costly weather disasters has led to an increased interest in understanding and quantifying severe weather events (e.g., Vose et al. 2014; Kunkel et al. 2013). For the northeast region of the United States (US), the most frequent cause of extreme wintertime weather is extratropical cyclones, which can create damage through their precipitation (Kunkel et al., 2012) and their winds (Ashley and Black, 2008). In view of this, the study herein seeks to understand the connection between strong wintertime surface wind events and extratropical cyclones in the Northeast United States.

Extratropical cyclones can approach the northeast US from the west, from the southwest and from the south, the latter of which are referred to as nor'easters. Several aspects of these wintertime storms have been discussed in the scientific literature. Miller (1946) separated nor'easters based on their genesis regions, drawing a distinction between those that originate over the Gulf of Mexico and those that develop over the Atlantic. Reitan (1974) estimated the most frequent paths of storms for 1951-1970, distinguishing paths for storms over the northeast US as: from the west, from the southwest, from the southeast and over the ocean (Fig. 12a in Reitan (1974)). Hirsch et al. (2001) developed a climatology of east coast winter storms, and included a strong wind threshold in their criteria for defining the storms. Dolan and Davis (1992) show that nor'easters tend to cause strong beach erosion events due to the westward direction of the winds poleward of the storm center, while Bernhardt and DeGaetano (2012) report on how the North Atlantic Oscillation and El Nino-Southern Oscillation relate to the storms that cause storm surge. However, less attention has been given to storms causing strong wind events over land in the Northeast US.

Vose et al. (2014) review the trends in wind events in the US, and find that available surface datasets and reanalysis products disagree on the sign of the trend (their Fig. 3, and Pryor et al. 2009). Similarly, Knox et al. (2011) review the current understanding of non-convective wind events, and suggest that there is some debate regarding the mechanisms causing high-wind events in extratropical cyclones. For instance, some case studies suggest that downward momentum mixing associated with tropopause folds may be responsible for high-wind events (e.g. Iacopelli and Knox 2001; Browning 2004), while other case studies find a key forcing from isallobaric winds (e.g., Durkee et al. 2012). However, the sting jet events discussed in Browning (2004) are rare, and the work on case studies over land (Fink et al., 2009; Gatzen et al., 2011; Durkee et al. 2012; Ludwig et al., 2015) suggest a more prominent role for ageostrophic fluxes.

Studies of strong surface wind in regions of the northeast United States have examined the most likely wind direction during an event. For instance, Niziol and Paone (2000) used station winds in western New York to show that the winds tend to be directed from the southwest to northeast during the strong events. For the Great Lakes region, Lacke et al. (2007) found a similar southwesterly propensity for the wind direction of strong, non-convective events (identified using weather reports) in which they defined strong events using the National Weather Service (NWS) criteria for high-wind watch or warning (sustained winds greater or equal to 18 ms^{-1} for 1 hour or a gust greater or equal to 26 ms^{-1} for any duration). Lacke et al. (2007) also found that the non-convective high wind events occur slightly more often in March and April, as compared to November-February. Most recently, Pryor et al. (2014) found spatial coherence over distances of up to 1000km in strong surface wind events, which, as they point out, implies synoptic systems create the wind events.

For Europe, far more attention has been given to windstorms in the literature, with studies that examine surface observations (Seregina et al., 2014) and reanalysis (Pinto et al., 2007; Leckebusch et al., 2008; Donat et al., 2010; Nissen et al., 2010; Pfahl, 2014; Roberts et al., 2014), global climate models (Knippertz et al., 2000; Della-Marta and Pinto, 2009), case-studies (Fink et al., 2009; Gatzen et al., 2011; Ludwig et al., 2014) as well statistical models (Schwierz et al., 2010; Haas and Pinto, 2012; Born et al. 2012; Pinto et al. 2012). Leckebusch et al. (2008) developed a method for identifying windstorms in gridded data, termed "footprinting". The technique detects winds that exceed a local threshold and then looks for spatial clusters of exceedances and tracks the clusters in time. Using this method, Leckebusch et al. (2008) established that high wind events associated with extratropical cyclones tend to occur to the south/southeast of the cyclone center, either along the cold front or slightly ahead of it. Nissen et al. (2010) used the same technique to show that a similar spatial arrangement exists for high wind events over the Mediterranean. These results for Europe, coupled with the work in the northeast US (Niziol and Paone, 2000; Lacke et al., 2007) suggest that associating extratropical cyclones with high wind events in the northeast US should identify a predominance of storms with their centers to the north/northwest of the wind events.

With this in mind, the present study will examine northeast US strong wind events and associate them with extratropical cyclone tracks. A goal of this work is to test if the results from Europe, that the location of the strongest winds occur southeast of the storm center, apply in the Northeast US. We analyze station based wind data from the Daily Summaries of the National Oceanic and Atmospheric Administration (NOAA) Integrated Surface Database (Smith et al. 2011), a quality-controlled, surface-station dataset. To maximize the likelihood of studying extratropical cyclones, we only examine winds that occur in December through February (DJF).

Our analysis begins with an examination of high wind events in the northeast US and then turns its focus to those storms identified as creating the strong wind events. To categorize the strong wind events, this study uses a probabilistic approach, following Della-Marta and Pinto (2009). Once identified strong wind events are associated with extratropical cyclone tracks, as for example in Yarnal (Chapter 6 (1993)), to identify the pathway of the storms that are associated with strong winds in the northeast US. After identifying the most likely pathway for the storms, we test the robustness of the pathway results.

2. Data and Methods

2.1 Data

This study uses the Daily Summary Data from NOAA's Integrated Surface Database (ISD). The ISD consists of global, synoptic observations compiled from surface weather observation stations, ranging from airports to military bases. The Daily Summary dataset is a quality-controlled subset of the ISD provided by NOAA. The key variable we examine is the sustained wind maximum, which NOAA defines as the daily maximum of the 2-minute averages from each hourly observation reported for the day (personal communication, Mark Lackey, NOAA). Here we refer to this variable as MAX. We focus the analysis on the sustained wind maximum rather than the wind gust because the MAX data are more frequently available for our study period and region. We also use the daily mean wind speed (MEAN), defined as the 24-hour average wind speed, which is also provided as part of the Daily Summary. The data are reported in whole knots, which results in the data being quantized (with an approximate interval of 0.5 ms^{-1}) rather than continuous (Pryor et al. 2009). We note that the Daily Summary dataset does not include wind direction, and therefore it is not considered in this study.

Our analysis focuses on the Northeast Region as defined by NOAA, which consists of 12 states: West Virginia, Maryland, Pennsylvania, Delaware, New Jersey, New York, Connecticut, Rhode Island, Massachusetts, Vermont, New Hampshire, Maine. For these states, we use all of the ISD stations for which at least 80% of MAX data are reported during DJF for the period from January 1979 to December 2012, which yields 49 stations (Fig. 1a). We choose January 1979 as the start date for our analysis because it coincides with the beginning of the reanalysis data used to identify extratropical cyclones (see Section 2.3). A table that lists all station names, locations and the percentage of data available is provided in the supplementary material (Supplemental Table S1).

We choose a cut-off of 80% data coverage to establish broad station coverage over the entire study region, which allows for a synoptic scale analysis. To test that this amount of data coverage yields robust results, we performed two sensitivity analyses: (1) we repeated the main analysis reported in Section 3 using only stations with 90% or more data coverage, (2) we tested if missing data at a given station occurs more often when a high wind event occurs at one or multiple other stations within 250 km. Neither analysis indicated a systematic bias, suggesting that this set of 49 stations provides a representative synoptic view for winds in the northeast US.

Before analyzing the data, we took additional steps to address other potential biases. First, we removed any sustained wind maximum data for which the concurrent mean wind speed data are zero (dubious data). Second, any sustained wind maxima that were found to be suspiciously larger than the concurrent mean wind for that day have been removed. To accomplish this, we define a new variable, η, for each station i:

$$\eta_i(t) = \frac{MAX_i(t) - MEAN_i(t)}{\sum_{j=1}^{N} MAX_j(t) - MEAN_j(t)} . \quad (1)$$

In the denominator, we average over the N stations within 250 km of station *i*, not including station *i*. If η is large, then the difference between the MAX and MEAN at station *i* is large, as compared to the difference between MAX and MEAN for the surrounding stations. We chose to remove any data for which η was larger than 4, which led to a removal of overall less than 0.002% of the original data, or 172 total data points.

The data removed using the η threshold, are, by definition of η, isolated winds events. However, some of the data removed are strong winds, which might suggest this method is removing important data. However, 168 of the 172 WMAX data removed using η occur prior to Jan 1, 1999 (Supplemental Figure S1). This date corresponds to the near completion of the transition to the ASOS observing systems (McKee et al. 2000), which meant the majority of the manual reporting was replaced by electronic reporting. McKee et al. (2000) note that the speed and direction were similar for manual and ASOS, but there were issues with the gust measurements, due to differences in the measurement-averaging window of the devices. Hayes and Kuhl (1995) note a difference in the reporting of peak wind events, due to differences in thresholds for defining peak winds. These biases would not affect our results, because we do not focus on gusts or the count of peak wind reports. On the other hand, the fact that such a high percentage of data identified using η occurred prior to 1999 suggests that the data removed because $\eta > 4$ may indeed be erroneous. For our purposes of associating multi-station wind events with extratropical cyclones, the removal of the data with large η is justified.

2.2 Identifying High Wind Events

The classification of high wind events (HWEs) that will be utilized in this study is a probabilistic approach following statistical extreme value theory (EVT) (e.g., Coles, 2001; Coles and Pericchi, 2003; Davison and Smith, 1990). For the identification of HWEs we use a peak-over-threshold (POT) model for MAX, based on the generalized Pareto distribution (GPD). Asymptotic arguments (e.g., Pickands, 1975) justify the use of the GPD for modeling exceedances over a high (enough) threshold because the GPD is the limiting distribution of a normalized exceedance over a threshold as the threshold approaches the maximum of the distribution (e.g., Coles, 2001). The GPD is defined as:

$$F(x) = 1 - \left[1 + \xi \frac{x-\mu}{\sigma}\right]^{-\frac{1}{\xi}}, \sigma > 0, x > \mu, 1 + \xi \frac{x-\mu}{\sigma} > 0, \qquad (2)$$

where x are daily data (here MAX), u is the threshold value and σ and ξ are the scale (a measure of the spread of the distribution of x) and shape parameter (which is determining the shape of the distribution, rather than shifting it as u does or shrinking/stretching it as σ does), respectively. In the GPD framework an essential step is to determine a threshold u for which the asymptotic GPD approximation holds. Threshold choice involves a trade-off between bias and variance as: (i) a too high threshold will reduce the number of exceedances and increase the estimation variance; while (ii) a too low threshold will induce a bias as the GPD will poorly fit the exceedances.

In this study we use the POT-package (Ribatet, 2007) within R for the EVT analysis. In this package the GPD parameters (σ and ξ) are computed by maximum-likelihood estimation. Evaluation of the GPD fit at the 49 northeast US sites considered here show that the 97-th quantile provides a suitable threshold choice at all sites, satisfying the trade-off between bias and variance. Supplemental Figure S2 provides an exemplary comparison of results from GPD fits at selected sites with too high and too low threshold values.

Supplemental Figure S3 shows the probability density functions (PDFs) of wintertime MAX from the 49 northeast US sites in the ISD that fulfill the data selection criteria outlined in Section 2.1. The PDFs are asymmetric with heavier upper tails. We note that a similar skew was found in the PDFs of surface winds using the entire year, rather than DJF (He et al. 2010), and similar statistics were found in Pryor et al. (2014). Figure S3 also shows that the winds exceeding the threshold for a high wind watch or warning for the NWS (days with MAX > 18 ms^{-1}) represent the upper end of the PDF range and occur very rarely.

Next we analyze the winds from two stations to illustrate why we have chosen to use probabilistic statistics. The top panels of Figure 2 show the observed MAX (y-axis) versus the estimate from a Gaussian fit (x-axis) for two selected (and representative) sites in the northeast US: Bridgeport, Connecticut (left column) and Elkins-Randolph County, West Virginia (right column). The figures confirm that the tails of MAX are non-Gaussian (i.e., data from a Gaussian distribution would lie close to the diagonal 1:1 line). The grey-hashed boxes in the top panels (a and b) in Figure 2 give the data range at the two selected sites beyond the 97-th quantile. The middle panels (c and d) of Figure 2 (which are a zoom-in on the grey, hashed boxes of the top panels) show observed (y-axis) versus GPD-fitted (x-axis) MAX. Comparing the top and middle panels in Figure 2 shows that the GPD provides a better fit compared to a Gaussian distribution.

After fitting the GPD ($F_{\xi,\mu,\sigma}$), we calculate the empirical return level (R^T) as:

$$R_T = F^{-1}_{\xi,\mu,\sigma}\left(1 - \frac{1}{T}\right). \tag{3}$$

Return levels are of practical interest because they describe the probability of exceeding a value *x* within a time window T. The bottom panels of Figure 2 show return level plots for the two selected sites. Thus, for example, MAX > 18 ms^{-1} at the Bridgeport site would have a probabilistic 5-year return level, while at the Elkins-Randolph County site it would have a probabilistic return level of more than 20 years.

For the purpose of this study we choose to use 1-year, 3-year and 5-year return levels to define HWEs. The reason being twofold: (i) return levels accurately capture the tail properties of MAX; (ii) they provide a comparable standardized metric for MAX across individual sites. Using HWEs at each station, we identify simultaneous exceedances of multiple station return levels (hereafter, multi-station events) by finding all HWEs that occur on the same date +/- 1 day. The window of +/- 1 day accounts for the possibility that a storm caused HWEs on either side of 0Z (i.e., two different days in the daily summary), and the possibility of the same storm transiting the study region over a 2-day period. We define the center of a multi-station event as the average of latitude and longitude positions of the stations reporting the event.

2.3 Extratropical Cyclone Association

Extratropical cyclones are identified by tracking their low-pressure centers, using 6-hourly sea level pressure (SLP) fields from the European Center for Medium Range Forecasts (ECMWF) ERA-Interim reanalysis (Dee et al. 2011). ERA-Interim has been shown to compare favorably with other reanalysis data for cyclone tracking (Hodges et al. 2011). To account for possible biases in the trackers (e.g. Neu et al., 2013), we performed our analysis using two separate cyclone-tracking algorithms: TRACK (Hodges, 1999) and the MAP Climatology for Midlatitude Storminess (Bauer and Del Genio 2006). Despite major differences in the design of the tracking algorithms, we found similar results in the wind analysis for both. Therefore we present in the remainder of the paper only results based on the Hodges tracking scheme.

For the track database, we include tracks that last for at least 48-hours and travel at least 1000 km, which allows focusing on mobile synoptic systems. Figure 1b shows the track density for all storms that pass through a box over the northeast region (Fig. 1b, black, dashed box). The box used is sufficiently larger than the region of the stations so that the storm set includes all storms that might influence the area. The track density is a count of the tracks per 2° by 2° grid box per winter (DJF). The pattern shows a maximum over the Gulf Stream and a secondary maximum over the Great Lakes, in good agreement with the pattern reported for east coast wintertime storms in previous work (Hirsch et al. 2001). For DJF, from 1979-2012, for tracks passing through the box in Figure 1b, we find a total of 1034 storms.

To associate the cyclone tracks with multi-station wind events, we require that the cyclone center be within 1500 km of the geographical center of the event (see end of Section 2.2 for the definition of a center of a multi-station event). We have tested other radii, i.e., 1000 km, and found that the smaller distance excludes obvious storms. Since the track data are 6-hourly, while the station data are daily, we consider any cyclone that is within 1500 km at the time of the event +/- 12 hours. For the multi-station events that occur on a single day, we use 12Z for that day. For the events that span two days, 0Z on the latter day is used.

In the cases in which multiple storms are found in proximity (in time and space) of the wind event, wind direction data from the ERA-Interim reanalysis are used to identify the most likely related storm. For this, first the area average of the 925-hPa zonal and meridional winds over a 5° by 5° region centered on the multi-station event is calculated. Second, wind direction is calculated from the area-averaged winds. If the wind direction has a northerly component, we retain the cyclones east of the station event (i.e., the winds are part of the back-end of the storm), and vice-versa for winds with a southerly component. For the rare case that there are still multiple storms that fulfill the selection criteria, the storm that is closest in space to the wind event is kept.

3. Results

3.1 Extratropical Cyclone Tracks for Multi-Station HWEs

The HWEs during DJF in the northeast United States are defined by identifying wind events that exceed the station-specific 1, 3 and 5-yr return levels (Table 1). We then find the dates on which multiple stations have HWEs, hereafter, multi-station events. Table 1 shows the results for exceedances of the 1-, 3-, and 5-year return levels, with the number of events occurring simultaneously at multiple stations decreasing as the number of stations increases, though not monotonically. The analysis that follows will mainly focus on multi-station events for which 3 or more stations exceed their 3-year return levels. There are 52 of these events (i.e., 13+8+6+8+17, using the data on the 3-year return level row in Table 1). Analysis will also be carried out on multi-station events for which 5 or more stations exceed their 5-year return periods, for which there are: 15 (i.e., 6+4+5, using the data on the 5-year return level row in Table 1) events.

Isolated events are defined as the dates for which only one station exceeds the given return level and these occur most frequently. As shown in Column 3 of Table 1, the occurrence of isolated events greatly reduces if 1-year return levels for surrounding stations are considered. For example, if the simultaneous exceedances of 5-year return levels are considered, then 85 single-station exceedances of the 5-year levels are found. However, if we consider simultaneous exceedances of 1-year and 5-year levels, the number of single-station exceedances of the 5-year levels drops significantly, down to 28. For reference, the dates for multi-station events defined as

5 or more stations with exceedances of the 5-year levels are listed in Supplemental Table S2. Some of these storms were deadly (see for instance, Asuma 2010).

Using the extratropical cyclone association technique described in Section 2.3, we associate each multi-station event with a cyclone track, when possible. Figure 3 shows examples of this for multi-station events in which 3 stations simultaneously experienced winds that exceeded their 3-year return levels (Table 1). In this case, cyclones were associated with 11 of the 13 multi-station events. The figure shows that in some cases a multi-station event is based on 3 stations in close proximity (e.g., Dec 21, 2012 in Fig. 3b), while in other cases the stations are spread across the region (e.g., Dec 29, 1994 in Fig. 3a).

Next, we examine the associated tracks when using different thresholds to define a multi-station event (Fig. 4). Figure 4a shows the tracks for all events for which there are at least 5 stations at which the wind exceeded the station's 1-year return level. There are 102 multi-station events that fit the definition and for 82 of these events an associated cyclone is identified. In this case, no preferred path is obvious, perhaps due to the large number of tracks included in the plot. Figure 4b shows the paths for multi-station events defined as exceedances of the 3-year return level at 3 or more stations. There are 52 events that fit this definition, and for 44 of these events an associated cyclone is identified. In this case, there appears to be more storms that arrive in the northeast region from the west or southwest. Figures 4c and 4d show results for more stringent definitions of multi-station events, and a higher percentage of events are associated with a cyclone track that arrives in the northeast from the southwest. For the multi-station events defined as 5 or more stations exceeding their 3-year return level, 31 events are found with 26 associated cyclone tracks. For the multi-station events defined at 5 or more stations exceeding their 5-year return level, 15 events are found with 13 associated cyclones identified.

Figure 5 shows, for different thresholds used to define a multi-station event, the location of the storm center (in red) and the location of the average of the latitude and longitudes for the stations with HWEs in the event (in blue). For each of these definitions, the majority of the storm centers are north or northwest of the stations experiencing a wind event, suggesting that the winds are in the south/southeast quadrant of the cyclones. Consistent with this result, a composite of the SLP field for the study domain (using ERA-Interim reanalysis) on the day of the multi-station events, based on 5 or more stations exceeding the 5-year return levels, also shows the storm center north of our study region (Fig. 6). The SLP contours further suggest that the winds are directed from the southwest to the northeast, which is in agreement with the individual station studies of Niziol and Paone (2000) and Lacke et al. (2007).

3.2 Quantifying the Preferred Extratropical Cyclone Path

The qualitative results from the previous section show a preference for the multi-station events being caused by storms approaching from the southwest. Next, we quantify this preference by examining the relative occurrence of strong wind associated storms arriving from different directions. To do this, a new methodology for separating the cyclone tracks based on their initial locations and paths is presented. Then the technique is applied to all cyclone tracks in the northeast US and to the tracks associated with multi-station events.

Motivated by the track separation presented in Reitan (1974), we have designed an analysis aimed at separating the cyclone tracks into those that take a zonal path towards the northeast US, those that arrive from the SW, and those that move northward along the coast. The analysis utilizes knowledge of the tracks initial development region and their trajectory across the northeast US. We use a reference frame centered at the geometric average of the latitude and longitude positions of the 49 weather stations to draw a crosshairs based on fixed lines of latitude (41.37° N), and longitude (75.06° W), which hereinafter are referred to as latFIX and lonFIX for simplicity. The storms are then separated into four groups:

(1) fromNW: tracks that begin northwest of the intersection and remain north of latFIX.
(2) fromSW: tracks that begin southwest of the intersection and either remain in that quadrant or cross latFIX traveling north to the west of lonFIX.
(3) fromSE: tracks that cross lonFIX traveling east to the south of latFIX.
(4) overOCEAN: tracks that remain east of lonFIX or cross lonFIX traveling west.

We note that many of the storms in the fromSE and overOCEAN tracks could be considered nor'easter's based on the wind pattern they generate when passing the northeast US. However, the classification used here does not include nor'easters as an individual category, because the paths have been separated based on their origin.

Panels (a)-(d) in Figure 7 show the track density (using the same procedure as in Fig. 1b) for the full storm set, based on these categories. For this separation, we find that if we consider all events there is a relatively equal number of tracks per characteristic path (Table 2). To test the sensitivity of the separation in respect to the values of lonFIX and latFIX, we repeat the analysis, shifting the location of the reference frame center by one degree in each direction (Table 2). As expected the results show that counts change with shifts, however this does not result in any drastic changes.

Next the track separation technique is used to parse the tracks associated with the multi-station events. For this analysis, we use the tracks found based on events for which the winds exceed the 3-year return level at 3 or more stations (i.e., Fig. 4b). Panels (e)-(h) in Figure 7 show these tracks separated into the characteristic pathways, with the counts as follows: fromNW (7), fromSW (27), fromSE (9), overOCEAN (1). Using the number of total storms per characteristic track found (given in Table 2), the relative frequency of storms causing multi-station events per characteristic path is calculated. For fromSW the value is 10.5%, which is at least three times greater than any of the frequencies for the other pathways. Furthermore, given that each of the 4 pathways have nearly the same number of tracks when all of the extratropical cyclones are considered (Table 2), we can use binomial probabilities to test the significance of the strong wind path result. In particular, if we consider this a Bernoulli Experiment and use the binomial distribution to test the likelihood of 27 of the 44 events coming from one pathway. The probability is less than 1 in a million.

To conclude this section, we discuss our choice for extratropical pathway separation. The crosshairs separation technique used is subjective and based on prior understanding of the likely pathways that storms take to arrive in the northeast US (e.g., Reitan 1974). In an attempt to make a more objective track separation the tracks separated were also using hierarchical clustering (Ward 1963), a technique that has been previously applied to atmospheric circulation regimes (e.g. Casola and Wallace 2007). The clustering analysis resulted in a similar set of final clusters, i.e. the characteristics paths, as those we found using the crosshairs. However, the number of tracks per final cluster was very sensitive to the geographical extent of the tracks that was fed into the clustering algorithm. The clustering algorithm does not provide a simple mechanism for showing the sensitivity of the track separation to slight changes in the method, as we did here for the crosshairs method with Table 2. This led us to conclude that our technique, though subjective, offers the simplest and most easily reproducible method for separating the tracks.

3.3 Robustness of the Preferred Extratropical Cyclone Path

This section details two analyses designed to test the robustness of the preferred pathway result. First, the sensitivity of the pathway analysis to the geographical density of the surface stations is evaluated. Second, we test if the pathway analysis is sensitive to the number of stations within range of the cyclone winds.

To test if the existence of a denser concentration of stations along the coast versus inland (see Fig. 1a) creates a bias, we repeat the storm association analysis using a subset of stations that are more evenly spaced. To this aim we retain only one station separated by a 100-km radius, which results in a subset of 23 stations (Fig. 1a; yellow crosses). Using the 23-station subset, we find 27 multi-station events defined based on at least a 3-year return level at 3 or more stations (as opposed to the 52 multi-station events found using the full set). For these 27 events, we find 23 associated tracks, and the track separation of the storms again results in fromSW again being the most likely pathway (Supplemental Fig. S4). For further sensitivity analysis we repeated the analysis using radii of 50 km and 150 km (to create more regularly spaced station data sets) and found results consistent with those presented based on the 100-km radius. Thus, the results show that the geographical density of stations does not affect our results

Given the location of the stations relative to the paths of the cyclones centers, one could argue that the fromSW pathway being the most likely to cause multi-station events is a result of there being more stations within range of the cyclone winds that take this path. To test this hypothesis, we repeat the track association analysis using HWEs identified in the wind field in the ERA-Interim reanalysis using a fixed location. The idea behind this analysis is to utilize the temporal and spatial continuity of the reanalysis data in order to identify high wind events similar to the scale found using the multi-station approach at a single, fixed location.

For the region within 77.5˚ W to 70˚ W by 40˚ N to 43˚ N (red box in Fig. 8a), the 3 strongest values of the, 925-hPa daily-averaged windspeed from ERA-Interim are identified and averaged to a single value. Then the DJF values in the resulting time-series are fit to a GPD. Because the 925-hPa daily-averaged wind speed represents a smoother distribution with less striking extremes compared to the ISD observations, we focus on shorter return levels (i.e., 1 year or above) to establish robust statistics. We identify the high-wind events as those that exceed the 1-year return level and then isolate events that are at least 3 days apart (to remove the chance of double counting a storm). If multiple exceedances of the 1-year return level occur within 3 days, the strongest event is used. These HWEs are then associated with extratropical cyclones using the method described in Section 2.3.

Figure 8a shows the tracks associated with 925-hPa HWEs using the black box shown in the figure. In this case, as for the ISD multi-station events, most of the tracks travel from the southwest. To test if this characteristic pathway is caused by coastline geometry or topography, we repeat the analysis using two other boxes at the same latitude, east of the first box (Fig. 8b, 8c). In these cases we test for associated storms using a set of cyclone tracks that includes more storms over the ocean, which are not necessarily included in the original set of 1034 storms. Once again, the tracks that create high wind events for each region tend to be those that approach the box from the southwest. These results suggest that the identification of the fromSW pathway in the station analysis is unlikely to be based on which track passed over the most stations. These results also have implications for the cause of the fromSW pathway being the dominant track for wind events in the Northeast, related to the location within cyclones where the strongest winds occur. This is discussed in Section 4.

3.4 Geographical Distribution of High Wind Return Levels

For the EVT-based HWEs, we also examine the geographical climatology of events in the northeast US by plotting the average wind speeds for the 1-, 3- and 5-year events, per station (Fig. 9). The three panels show that the average strength of HWEs at stations near the Great Lakes and stations along the coast are usually larger than those for inland stations. Given the results from Figure 9, we use the geographical locations of the stations to create four subsets of sites for the northeast: Great Lakes, Inlands, Near-Coast and At-Coast (Fig. 9, and Table S1 in the supplemental material for each station's designation). Station designation is defined in the following way. The Great Lakes stations are all stations within 100 km of any Great Lake. The At-Coast stations are all stations within 40 km of the coastline, while all stations between 100 km and 40 km from the coastline are classified as Near-Coast. We then calculate average wind speeds for the 1-, 3- and 5- year events for each of the subsets. The results show that winds are stronger near the Great Lakes and at the Coast. A detailed summary is presented in Table 3 serving as a first-order benchmark for the strength of wintertime high wind events in these regions of the northeast. We note that the distances used to separate the data are arbitrary and chosen to simplify the presentation in Table 3.

4. Discussion

The analysis reveals that storms taking a path from the southwest towards the northeast region are most likely to cause multi-station strong winds events in the region (Fig. 4). It appears that this is a result of the south by southeast quadrant of these storms being more likely to pass over the stations as compared to any of the other paths, as evidenced by the fixed location analysis of the reanalysis winds (Fig. 8). Figure 8 also shows that if we consider a region farther east, the dominant storms would be those from the nor'easters or fromSW categories for our 1034 storms. This, again, is because the east by southeast quadrant of those storms would be more likely to pass over that region. As such, our work does not imply that the fromSW storms create stronger winds than storms from the other groups, but that the strong winds generated by the storms taking the fromSW path are most likely to occur over the northeast US. This is consistent with an analysis of strong wind producing storms over western Europe (Ulbrich et al. 2001; Leckebusch et al., 2008; Nissen et al., 2010; Pfahl 2014), which find the cyclone centers tend to be north of the wind events, and the wind events tend to be in the warm sector near the cold front, or just behind the cold front. The locations of the strong winds relative to the storm center are also in accord with composite views of winds within extratropical cyclones (e.g., Bengtsson et al. 2009; Catto et al. 2010; Booth et al. 2013).

We also tested for a relationship between the strength of the wind events and the strength of the storms, based on the storm-centered SLP gradient (gradSLP), for each storm at the time of the wind event. In an analysis of the set of multi-station events for which the 3-year return levels are exceeded by 3 or more stations, we calculate the station-averaged windspeed and gradSLP for the associated storms. However, no correlation between the gradSLP and surface station winds for the multi-station events was found. This null result is somewhat expected. The SLP gradient provides a proxy for the geostrophic forcing of the surface winds, however, as shown in Fink et al. (2009) and Durkee et al. (2012), the surface winds also contain ageostrophic components. Because the strong winds occur in the proximity of the cold front of the storms, it is also possible that momentum mixing associated with convection also provides an ageostrophic forcing for the surface winds.

5. Summary

This study identified historical strong wintertime surface wind events in the northeast US using station data. We applied methods from statistical extreme value theory to calculate probabilistic 1-, 3- and 5-year return levels for surface weather stations and linked events that occurred on the same date to identify multi-station events. Using these multi-station strong wind events, the associated extratropical cyclones were identified. The main finding of the presented study is that storms approaching the region from the southwest are most likely to be associated with strong surface winds. Results of a track separation analysis of all cyclone tracks for 1979-2012 show that, a storm causing strong surface winds is more likely to approach from the southwest than any other direction.

Our findings regarding the strongest winds within the warm sector support and expand on results from multiple studies over Europe (e.g., Leckebusch et al. 2008 and Nissen et al. 2010). In particular, the present study confirms that for the northeast US, the Leckebusch et al. (2008) results regarding the relative location of the winds within the cyclone is the key for understanding the locations at which cyclones creates strong winds. Additionally, we here utilized a new technique to identify strong synoptic wind events using station data: our multi-station event approach. This technique is unique from the wind footprinting analysis Leckebusch et al. (2008) and Nissen et al. (2010) applied to reanalysis winds. Therefore, the consistent results regarding the associated cyclones suggest that both methods (ours using surface observations and theirs using reanalysis winds) are capable of identifying strong synoptic wind storms. Future work will directly compare the two techniques.

To conclude, we discuss some of the implications of our results for storm impacts. First, if we consider storm impacts in the current climate, we can conclude that the extratropical cyclones that are associated with the strongest wind events over land most frequently are not the same as those that cause storm surge (i.e., Nor'easters), as reported in Dolan and Davis (1992). Next, if we consider storm impacts in a warmer world, the implications of our work suggest that projecting changes in surface wind events will depend in the foremost on the track of the cyclones. Based on the study of Colle et al. (2013), global climate models (GCMs) project an increase cyclone tracks over the coastline and slightly inland. Based on our results, this suggests a possible increase in strong wind events if the GCM projected track changes are correct.

Acknowledgements

The data used for this research can be freely obtained from the National Oceanic and Atmospheric Administration's (NOAA) National Climatic Data Center in the daily summary files of the Integrated Surface Database and NOAA's National Weather Service for providing storm reports, as well ECMWF ERA-Interim Reanalysis, via their web portals. We thank Kevin Hodges and Mike Bauer for sharing their cyclone tracking code. JFB, DL and YK were partially supported by the Consortium for Climate Risk in the Urban Northeast (award NA10OAR4310212 from the NOAA RISA Program) and the Research Opportunities in Space and Earth Science ROSES-2012 NASA grant NNX14AD48G.

References

Ashley, W. S. and A. W. Black, 2008: Fatalities associated with nonconvective high wind events in the United States. *J. of Appl. Meteor. and Clim*. **47**, 717–725.

Asuma, J. V., 2010: Cool-season high-wind events in the Northeast U.S., M.S. Thesis, University at Albany, State University of New York, 117. http://cstar.cestm.albany.edu/CAP_Projects/Project17/JAsuma/Asuma_Total_4Oct10_Final.pdf

Bauer, M. and A. D. Del Genio, 2006: Composite analysis of winter cyclones in a GCM: Influence on climatological humidity. *J. Clim.*, **19**, 1652-1672.

Bengtsson, L., K. I. Hodges, and N. Keenlyside, 2009: Will extratropical storms intensify in a warmer climate? *J. Climate*, **22**, 2276-2301.

Bernhardt J. E. and A. T. DeGaetano, 2012: Meteorological factors affecting the speed of movement and related impacts of extratropical cyclones along the U.S. east coast, *Nat. Haz.*, **61**, 1463-1472.

Booth, J. F., L. Thompson, J. Patoux, K. A. Kelly, S. Dickinson, 2010: The signature of the midlatitude tropospheric storm tracks in the surface winds. *J. Clim.*. **23**, 1160-1174.

Booth, J. F., C. Naud, A. D. Del Genio, 2013: Diagnosing warm frontal cloud formation in a GCM: A novel approach using conditional subsetting. *Journal of Climate*, ***26***, 5827-5845.

Born, K., P. L. Ludwig, and J. G. Pinto, 2012: Wind gust estimation for mid-European winter storms: Towards a probabilistic view. *Tellus*, **64A**, 17471, doi:10.3402/tellusa.v64i0.17471.

Browning, K. A., 2004: The sting at the end of the tail: Damaging winds associated with extratropical cyclones. *Quart. J. Roy. Meteor. Soc.*, **130**, 375–399.

Carlson T. N., 1998: Mid-Latitude Weather Systems. American Meteorological Society, Boston, USA. 507 pp.

Casola, J.H., and J.M. Wallace, 2007: Identifying Weather Regimes in the 500-hPa Geopotential Height Field for the Pacific-North American Sector Using a Limited-Contour Clustering Technique. *Journal of Applied Meteorology and Climatology*, **46**, 1619-1630.

Catto, J. L., L. C. Shaffrey and K. I. Hodges, 2010: Can Climate Models Capture the Structure of Extratropical Cyclones?. *J. Climate*, **23**, 1621–1635.

Coles, S., 2001: An introduction to statistical modeling of extreme values. Springer, London, UK. 209 pp.

Coles, S., and L. Pericchi, 2003: Anticipating catastrophes through extreme value modeling. *Journal of the Royal Statistical Society Series C-Applied Statistics*, **52**, 405-416.

Davison, A. C., and R. L. Smith, 1990: Models for exceedances over high thresholds (with Discussion). *Journal of the Royal Statistical Society Series B*, **52(3)**, 393-442.

Dee D. P., and co-authors, 2011: The ERA-Interim reanalysis: configuration and performance of the data assimilation systems. *Quart. J. Roy. Meteor. Soc.*, **137**, 553-597.

Della-Marta, P. M., and J. G. Pinto, 2009: Statistical uncertainty of changes in winter storms over the North Atlantic and Europe in an ensemble of transient climate simulations. *Geophys. Res. Lett.*, **36**, L14703, doi:10.1029/2009GL038557.

Dolan R. and R. Davis, 1992: An intensity scale for Atlantic Coast Northeast Storms. *J. Coast. Res.*, **8**, 840–853.

Donat, M. G., G. C. Leckebusch, J. G. Pinto, and U. Ulbrich, 2010: Examination of Wind Storms over Central Europe with respect to Circulation Weather Types and NAO phases. *Int J Climatol* **30**, 1289-1300. doi:10.1002/joc.1982

Durkee, J. D., C. F. Fuhrmann, J. A. Knox, and J. D. Frye, 2012: Ageostrophic contributions to a non-convective high wind event in the Great Lakes region. *Natl. Wea. Dig.*, **36(1)**, 28-41.

Fink, A. H., T Brucher, V. Ermert, A Kruger, J. G. Pinto, 2009: The European storm Kyrill in January 2007: Synoptic evolution, meteorological impacts and some considerations with respect to climate change. *Nat. Hazards Earth Syst. Sci*., **9**, 405-423, doi:10.5194/nhess-9-405-2009.

Gatzen, C, T. Pucik, D. Ryva, 2011: Two cold-season derechoes in Europe. *Atmos. Res*., **100**, 740-748, doi:10.1016/j.atmosres.2010.11.015.

Haas, R., and J. G. Pinto (2012), A combined statistical and dynamical approach for downscaling large-scale footprints of European windstorms, *Geophys. Res. Lett*., **39**, L23804, doi:10.1029/2012GL054014.

Hayes, J. C., and S. C. Kuhl (1995), An initial comparison of manual and automated surface observing system observations at the Atlantic City, New Jersey International Airport., 26pp., NOAA Technical Memorandum, NWS ER-89.

He, Y., A. H. Monahan, C. G. Jones, A. Dai, S. Biner, D. Caya, and K. Winger, 2010: Probability distributions of land surface wind speeds over North America. *J. Geophys. Res.*, **115**, D04103, doi:10.1029/2008JD010708.

Hirsch M., A. T. DeGaetano, S. J. Colucci, 2001: An east coast winter storm climatology. *J. Clim.*, **14**, 882–899.

Hodges, K. I., 1999: Adaptive Constraints for Feature Tracking. *Mon. Wea. Rev.*, **127**, 1362–1373.

Hodges, K. I., R. W. Lee, L. Bengtsson, 2011: A Comparison of Extratropical Cyclones in Recent Reanalyses ERA-Interim, NASA MERRA, NCEP CFSR, and JRA-25. *J. Climate,* **24***,* 4888–4906.

Iacopelli, A. J., and J. A. Knox, 2001: Mesoscale dynamics of the record-breaking 10 November 1998 mid-latitude cyclone: A satellite-based case study. *Natl. Wea. Dig.*, **25 (1)**, 33–42.

Knox, J. A., J. D. Frye, J. D. Durkee, and C. M. Fuhrmann, 2011: Non-convective high winds associated with extratropical cyclones. *Geogr. Compass*, **5(2)**, 63-89.

Kunkel, K. E., D. R. Easterling, D. A. R. Kristovich, B. Gleason, L. Stoecker, R. Smith, 2012: Meteorological Causes of the Secular Variations in Observed Extreme Precipitation Events for the Conterminous United States. *J. Hydrometeor,* **13**, 1131–1141.

Kunkel, K. E., and Coauthors, 2013: Monitoring and Understanding Trends in Extreme Storms: State of Knowledge. *Bull. Amer. Meteor. Soc*., **94**, 499–514.

Lacke, M.C., J.A. Knox, J.D. Frye, A.E. Stewart, J.D. Durkee, C.M. Fuhrmann, and S.M. Dillingham, 2007: A climatology of non-convective wind events in the Great Lakes. *J. Climate*, **20**, 6012–6022.

Leckebusch, G. C., D. Renggli, U. Ulbrich, 2008: Development and application of an objective storm severity measure for the Northeast Atlantic region. *Meteorol. Z.* **17**, 575-587. doi: 10.1127/0941-2948/2008/0323

Ludwig, P., J. G. Pinto, S. A. Hoepp, A. H. Fink, S. L. Gray, 2015: Secondary cyclogenesis along an occluded front leading to damaging wind gusts: windstorm Kyrill, January 2007. *Mon. Wea. Rev.*, **143**, 1417–1437., doi:10.1175/MWR-D-14-00304.1

McKee, T. B., N. J. Doesken, C. A. Davey, and R. A. Pielke Sr. (2000), Climate data continuity with ASOS: Report for period April 1996 through June 2000, 82 pp., Colo. Clim. Cent., Fort Collins.

Miller. J. E., 1946: Cyclogenesis in the Atlantic coastal region of the United States. *J. Meteor.* **3**, 31-44.

Neu, U., and Coauthors, 2013: IMILAST – a community effort to intercompare extratropical cyclone detection and tracking algorithms: assessing method-related uncertainties. *Bull. Am. Meteor. Soc.*, 94:529-547, doi: http://dx.doi.org/10.1175/BAMS-D-11-00154.1

Nissen, K.M., G. C. Leckebusch, J. G. Pinto, D. Renggli, S. Ulbrich, U. Ulbrich, 2010: Cyclones causing wind storms in the Mediterranean: characteristics, trends and links to large-scale patterns. *Nat Hazards Earth Syst Sci* **10**, 1379-1391. doi:10.5194/nhess-10-1379-2010

Niziol, T. A., and T. J. Paone, 2000: A climatology of non-convective high wind events in western New York state, NOAA Tech. Memo, NWS ER-91, 36.

Pinto, J. G., Fr¨ohlich, E. L., Leckebusch, G. C., and Ulbrich, U.: Changing European storm loss potentials under modified climate conditions according to ensemble simulations of the ECHAM5/MPI-OM1 GCM, *Nat. Hazards Earth Syst. Sci*., **7**, 165–175, doi:10.5194/nhess-7-165-2007, 2007.

Pinto, J.G., M. K. Karreman, K. Born, P. M. Della-Marta, M. Klawa, 2012: Loss potentials associated with European windstorms under future climate conditions. *Clim Res.,* **54**, 1-20. doi:10.3354/cr01111

Pfahl, S., 2014: Characterising the relationship between weather extremes in Europe and synoptic circulation features. *Nat. Hazards Earth Syst. Sci.,* **14**, 1461-1475, doi:10.5194/nhess-14-1461-2014.

Pickands, J., 1975: Statistical-inference using extreme order statistics. *Annals of Statistics,* ***3(1)***, 119-131.

Pryor, S. C., R. J. Barthelmie, D. T. Young, E. S. Takle, R. W. Arritt, D. Flory, W. J. Gutowski Jr., A. Nunes, and J. Roads, 2009: Wind speed trends over the contiguous United States. *J. Geophys. Res.*, **114**, D14105, doi:10.1029/2008JD011416.

Pryor, S. C., R. Conrick, C. Miller, J. Tyell, and R. J. Barthelmie, 2014: Intense and extreme wind speeds observerd by anemometer and seismic networks: An Eastern U.S. case study. *J. App. Meteor. and Clim.,* **53**, 2417-2429.

Reitan, C. H., 1974: Frequencies of Cyclones and Cyclogenesis for North America, 1951–1970. *Mon. Wea. Rev.,* **102**, 861–868.

Ribatet, M., 2007: POT: Modeling Peaks Over a Threshold. *R News*, **7**, 34-36.

Roberts, J.F., A. J. Champion, L. C. Dawkins, K. I. Hodges, L. C. Shaffrey, D. B. Stephenson, M. A. Stringer, H. E. Thornton, B. D. Youngman, 2014: The XWS open access catalogue of extreme European windstorms from 1979 to 2012. *Nat. Hazards Earth Syst. Sci.*, **14**, 2487-2501. doi: 10.5194/nhess-14-2487-2014

Schwierz, C., P. Kollner-Heck, E. Zenklusen Mutter, D. N. Bresch, P.-L. Vidale, M. Wild, C. Schar, 2010: Modelling European winter wind storm losses in current and future climate. *Clim Change* **101**, 485-514. doi: 10.1007/s10584-009-9712-1

Seregina, L. S., R. Haas, K. Born, J. G. Pinto, 2014: Development of a wind gust model to estimate gust speeds and their return periods. *Tellus A* **66**, 22905. doi:10.3402/tellusa.v66.22905

Smith, A., N. Lott, and R. Vose, 2011: The Integrated Surface Database: Recent Developments and Partnerships. *Bull. Amer. Meteor. Soc.,* **92**, 704-708.

Ulbrich U, Fink AH, Klawa M, Pinto JG, 2001) Three extreme storms over Europe in December 1999. *Weather,* **56**, 70–80.

Vose, Russell S., and Coauthors, 2014: Monitoring and Understanding Changes in Extremes: Extratropical Storms, Winds, and Waves. *Bull. Amer. Meteor. Soc.,* **95**, 377–386.

Ward, J. H., Jr., 1963: Hierarchical grouping to optimize an objective function. *J. Amer. Stat. Assoc.*, **58**, 236–244.

Yarnal, B. 1993: Synoptic climatology in environmental analysis: a primer. Belhaven Press,London, UK. 105 pp.

Tables

Table 1: Count of HWEs and multi-station events

Return Level (years)	Total HWEs	Isolated Events (isolated at 1-yr RL)	Multi-station events on the same day by number of stations[a]						
			Two	Three	Four	Five	Six	Seven or more	***Max # of stations***
1	1621	172	58	42	24	18	22	62	***29***
3	490	116 (47)	27	13	8	6	8	17	***14***
5	289	85 (28)	16	11	10	6	4	5	***8***

[a] For each of the return levels, the count of multi-station events per number of stations does not monotonically decrease as the number of station increases. It does have a downward tendency, however, it also has a long tail, as indicated by the last column.

Table 2: Track counts per characteristic paths vs location of crosshairs
counts are listed as: fromNW/fromSW/fromSE/overOCEAN

	40.4°N	**41.4°N**	**42.4°N**
283.8°W	239/254/240/301	221/256/256/301	201/255/277/301
284.8°W	245/259/264/266	**225/258/285/266**	205/263/300/266
285.8°W	249/265/279/243	228/260/303/243	207/267/317/243

Table 3: Average Strength of Wind Events by region
MIN/MEAN/MAX (ms-1)

	Great Lake	Inland	Near-Coast	At-Coast
1- to 3-year RL	12.3	10.8	11.3	13.3
	16	**14.3**	**14.6**	**15.6**
	19.6	17	17.5	18
3- to 5-year RL	16.5	12.8	12.4	15.3
	18	**15.6**	**16.2**	**16.8**
	20.1	17.5	18	19.6

Figure Caption List

Figure 1: Stations (a) and track density (b). In (a) Locations of ISD stations in NOAA Northeast Region with at least 80% MAX data for DJF for 1979-2012 are shown. Color of stations corresponds to percentage of data available. Yellow x's show stations used for repeated analysis in which a set of more evenly spaced staions was used (i.e., 1 site within 100 km radius, see text for further explanation). In (b) track density for extratropical cyclones in DJF, based on tracks from the TRACK algorithm. Units: count per winter (CPW). Contour interval is 2.5 CPW. Thicker contours show 5 CPW and 10 CPW. Black box shows region through which all tracks must travel to be included in database.

Figure 2: (a) Quantile-Quantile (QQ) plot comparing observed MAX (m/s) at Bridgeport with a least-square fitted Gaussian. (b) As (a) but for Elkins-Randolph County. (c) QQ-plot comparing observed MAX from Bridgeport with GPD-fitted MAX, (d) as (c) but for Elkins-Randolph County. (e) Return level plot for Bridgeport from the fitted GPD in (c), (f) as (e) but for Elkins-Randolph County. Grey Hashed boxes in (a) and (b) mark the data range above the 97-th quantile at each site. Orange dashed lines mark the NWS threshold for a high wind watch or warning (i.e., 18 ms^{-1}) in all panels. Secondary axis in (a) and (b) show corresponding mean values (M) and standard deviations (σ).

Figure 3: Multi-station events and associated tracks examples: multi-station events for which the winds exceed 3-year return levels at exactly 3 stations. 13 multi-station events were identified for this criterion. For 11 of these events, an associated extratropical cyclone is identified. Cyclone

tracks are the lines; station locations are the dots. The associated tracks and stations are given in the same color. The green dot on each track shows the location of storm at date of multi-station event. The legend shows the full date extent of each track and date of multi-station event in parentheses. For the Dec 4, 1990 case, there are two stations nearly overlapping in the NYC region.

Figure 4: Track associated with multi-station events based on different criteria: (a) 1-year return level (RL) at 5 or more station; track count 84 (total events: 102), (b) 3-year RL at 3 or more stations; track count 44 (total events: 52), (c) 3-year RL at 5 or more stations; track count 26 (total event 31), (d) 5-year RL at 5 or more stations; track count 13 (total events 15). Track count gives the number of associated tracks and total events gives the number of multi-station events identified for each specified criterion.

Figure 5: Location of cyclone centers (in blue) and geographical average location of associated stations (in red) during multi-station events with: (a) 3-year return level (RL) at 3 or more stations, (b) 3-year RL at 5 or more stations, (c) 5-year RL at 5 or more stations. Dashed black lines connect station center to associated storm center. For reference, the black circle shows a distance of 1000 km from the geographical center of all of the stations.

Figure 6: Composite for multi-station events. Contours show SLP (hPa), shading shows wind speed at 925 hPa (ms^{-1}). Multi-station events here are defined as HWEs exceeding the 5-yr return level at 5 or more stations.

Figure 7: Separating tracks based on characteristic pathways: (a-d) track density for all tracks and (e-h) track paths for storms associated with multi-station events. Pathway names: (a) fromNW, (b) overOCEAN (c) fromSW and (d) fromSE. Contour interval in (a-d): thin lines: 1.25 counts per winter, thick lines: 2.5 counts per winter. For storms associated with multi-station events, track count per path: (e) 7, (f) 1, (g) 27, (h) 8. Multi-station events defined here as: 3 or more stations exceeding their 3-year return level. Dashed lines show crosshairs designated by the geometric mean latitude and longitude of the stations.

Figure 8: Cyclone track association for area average of 925-hPa reanalysis winds in black boxes: Latitude range for all boxes: 40˚N – 43˚N. Longitude ranges: (a) 77.5˚W-70˚W, (b) 67.5˚W – 60˚W, and (c) 57.5˚W – 50˚W. Red line indicates the cyclone tracks, blue dot marks location of cyclone at time of association with high wind event for the area-averaged wind in the box.

Figure 9: (a) 1-year MAX return level on site basis; (b)-(c) as (a) but for 3-year and 5-year return levels.

Figures

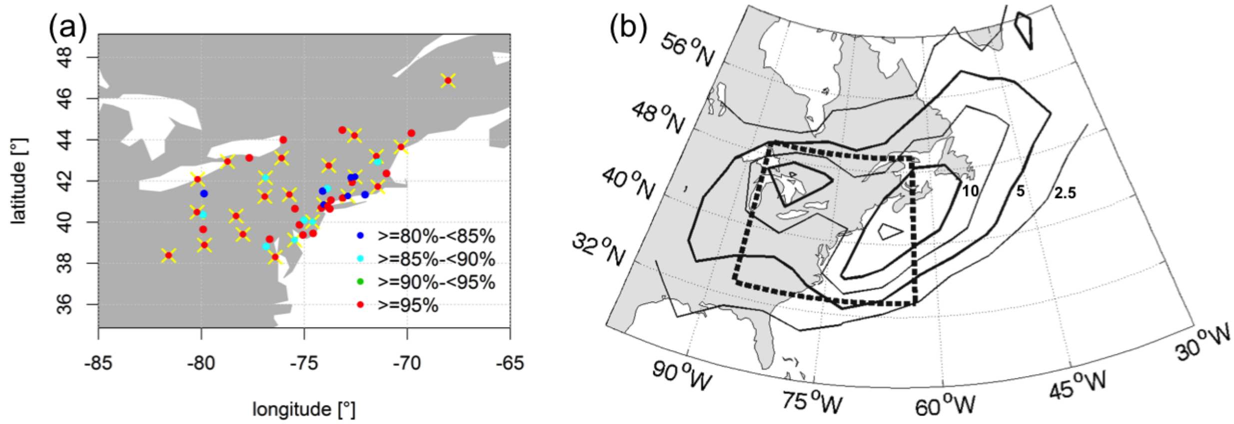

Figure 1: Stations (a) and track density (b). In (a) Locations of ISD stations in NOAA Northeast Region with at least 80% MAX data for DJF for 1979-2012 are shown. Color of stations corresponds to percentage of data available. Yellow x's show stations used for repeated analysis in which a set of more evenly spaced staions was used (i.e., 1 site within 100 km radius, see text for further explanation). In (b) track density for extratropical cyclones in DJF, based on tracks from the TRACK algorithm. Units: count per winter (CPW). Contour interval is 2.5 CPW. Thicker contours show 5 CPW and 10 CPW. Black box shows region through which all tracks must travel to be included in database.

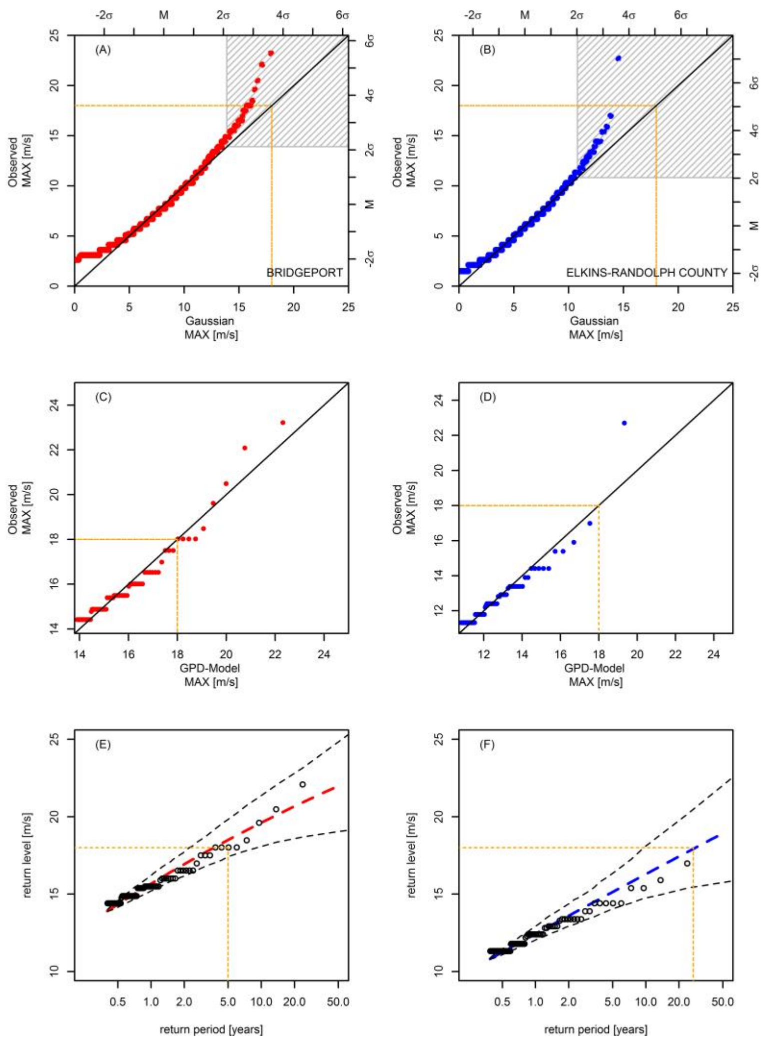

Figure 2: (a) Quantile-Quantile (QQ) plot comparing observed MAX (m/s) at Bridgeport with a least-square fitted Gaussian. (b) As (a) but for Elkins-Randolph County. (c) QQ-plot comparing observed MAX from Bridgeport with GPD-fitted MAX, (d) as (c) but for Elkins-Randolph County. (e) Return level plot for Bridgeport from the fitted GPD in (c), (f) as (e) but for Elkins-Randolph County. Grey Hashed boxes in (a) and (b) mark the data range above the 97-th quantile at each site. Orange dashed lines mark the NWS threshold for a high wind watch or warning (i.e., 18 ms^{-1}) in all panels. Secondary axis in (a) and (b) show corresponding mean values (M) and standard deviations (σ).

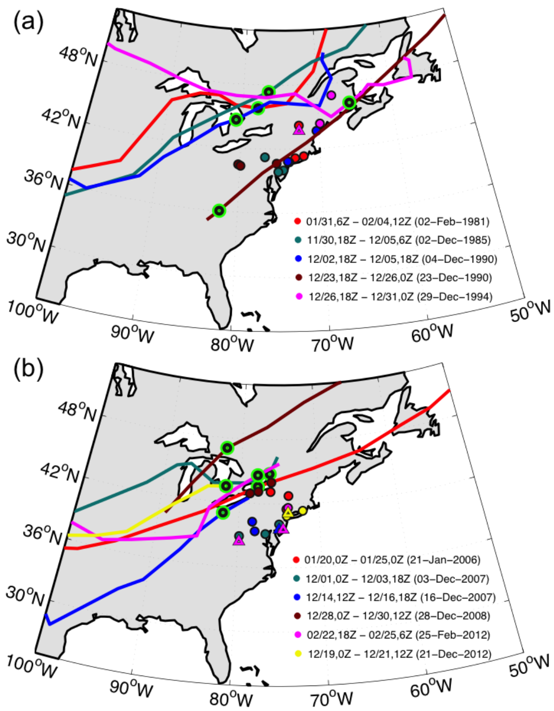

Figure 3: Multi-station events and associated tracks examples: multi-station events for which the winds exceed 3-year return levels at exactly 3 stations. 13 multi-station events were identified for this criterion. For 11 of these events, an associated extratropical cyclone is identified. Cyclone tracks are the lines; station locations are the dots. The associated tracks and stations are given in the same color. The green dot on each track shows the location of storm at date of multi-station event. The legend shows the full date extent of each track and date of multi-station event in parentheses. For the Dec 4, 1990 case, there are two stations nearly overlapping in the NYC region.

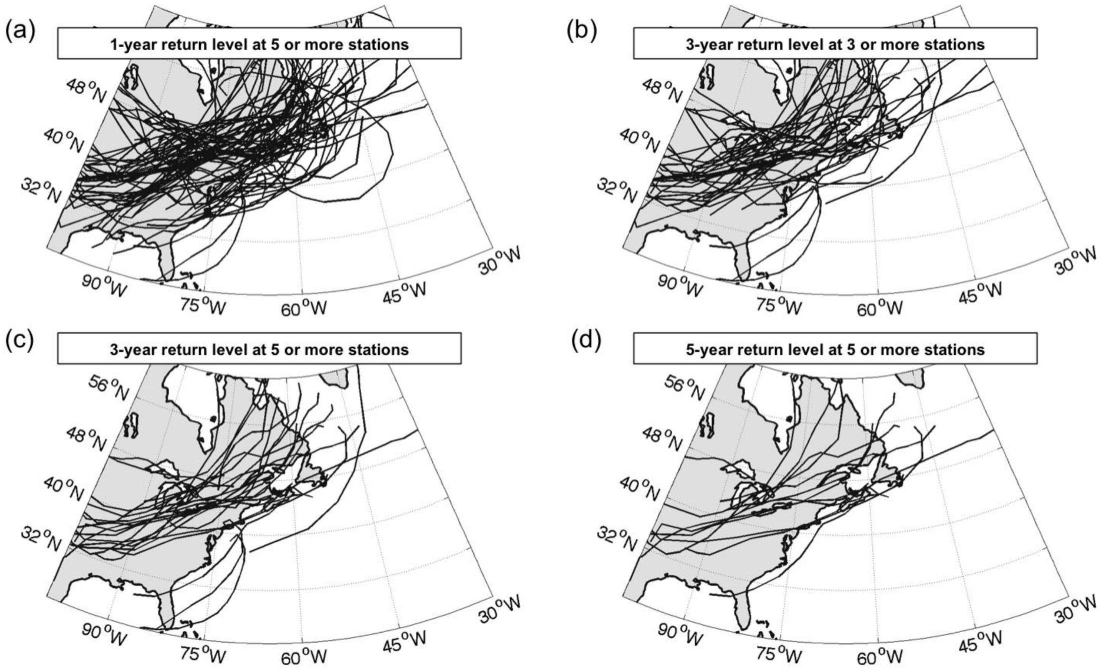

Figure 4: Track associated with multi-station events based on different criteria: (a) 1-year return level (RL) at 5 or more station; track count 84 (total events: 102), (b) 3-year RL at 3 or more stations; track count 44 (total events: 52), (c) 3-year RL at 5 or more stations; track count 26 (total event 31), (d) 5-year RL at 5 or more stations; track count 13 (total events 15). Track count gives the number of associated tracks and total events gives the number of multi-station events identified for each specified criterion.

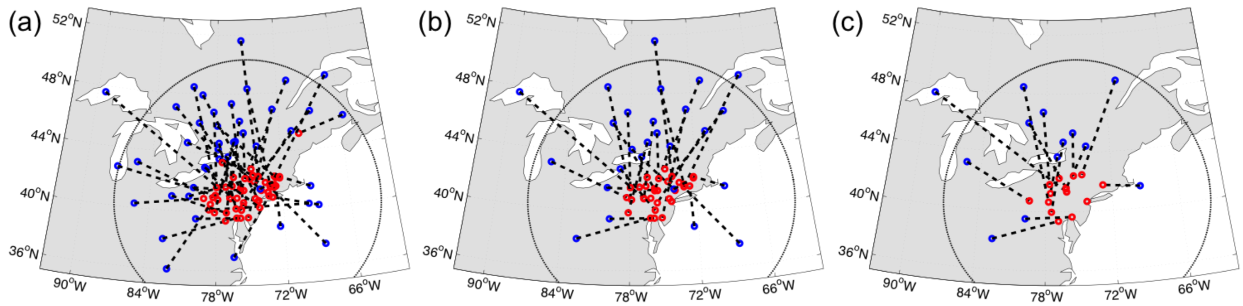

Figure 5: Location of cyclone centers (in blue) and geographical average location of associated stations (in red) during multi-station events with: (a) 3-year return level (RL) at 3 or more stations, (b) 3-year RL at 5 or more stations, (c) 5-year RL at 5 or more stations. Dashed black lines connect station center to associated storm center. For reference, the black circle shows a distance of 1000 km from the geographical center of all of the stations.

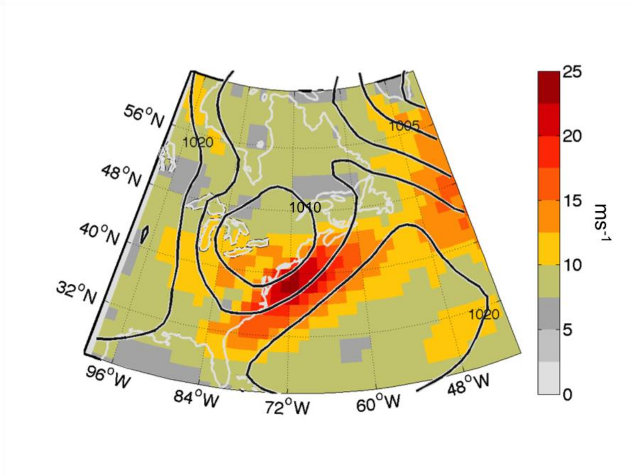

Figure 6: Composite for multi-station events. Contours show SLP (hPa), shading shows wind speed at 925 hPa (ms^{-1}). Multi-station events here are defined as HWEs exceeding the 5-yr return level at 5 or more stations.

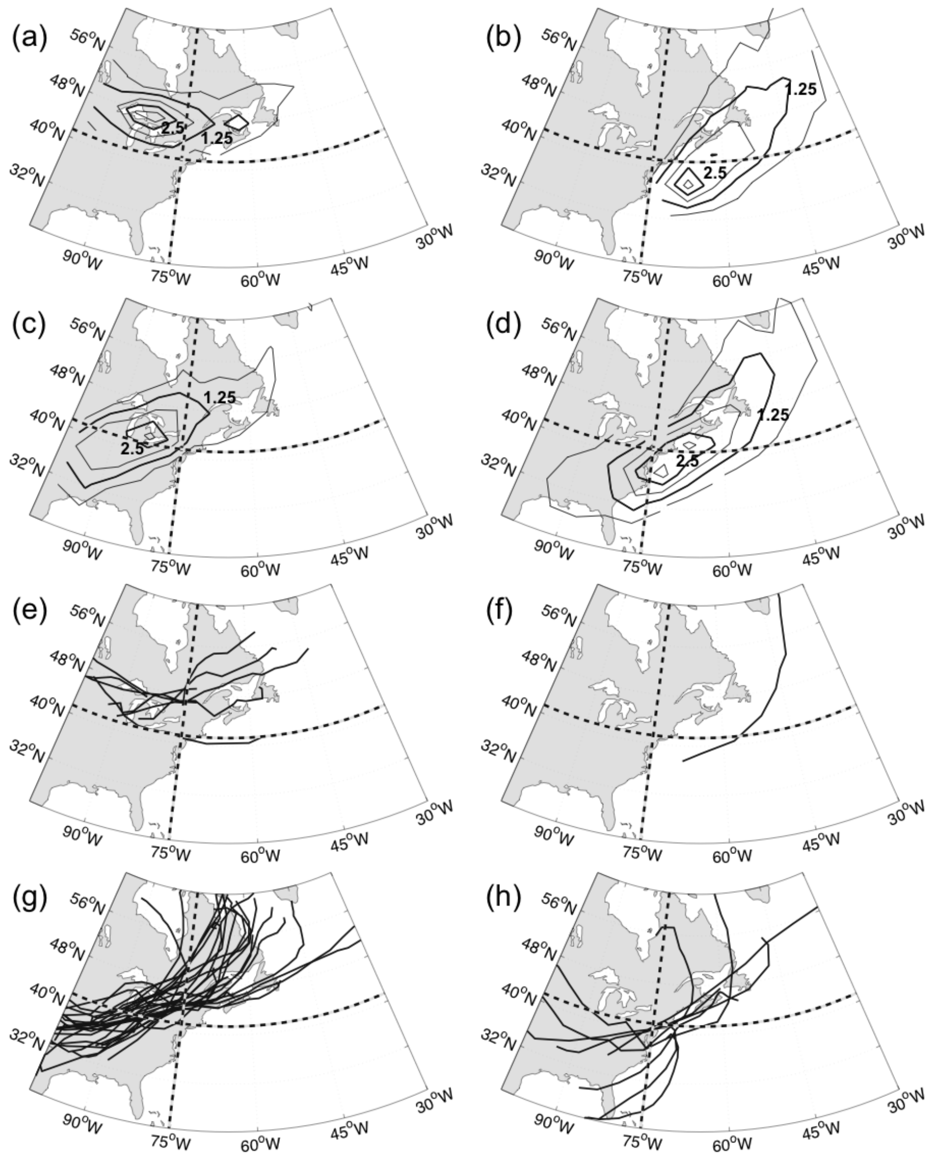

Figure 7: Separating tracks based on characteristic pathways: (a-d) track density for all tracks and (e-h) track paths for storms associated with multi-station events. Pathway names: (a) fromNW, (b) overOCEAN (c) fromSW and (d) fromSE. Contour interval in (a-d): thin lines: 1.25 counts per winter, thick lines: 2.5 counts per winter. For storms associated with multi-station events, track count per path: (e) 7, (f) 1, (g) 27, (h) 9. Multi-station events defined here as: 3 or more stations exceeding their 3-year return level. Dashed lines show crosshairs designated by the geometric mean latitude and longitude of the stations

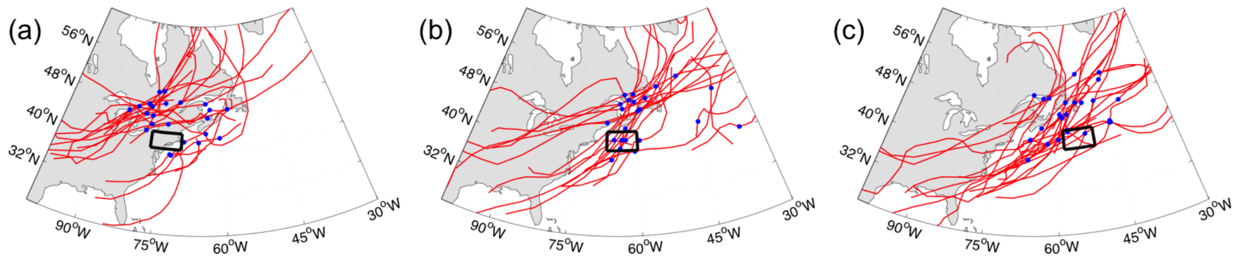

Figure 8: Cyclone track association for area average of 925-hPa reanalysis winds in black boxes: Latitude range for all boxes: 40˚N – 43˚N. Longitude ranges: (a) 77.5˚W-70˚W, (b) 67.5˚W – 60˚W, and (c) 57.5˚W – 50˚W. Red line indicates the cyclone tracks, blue dot marks location of cyclone at time of association with high wind event for the area-averaged wind in the box.

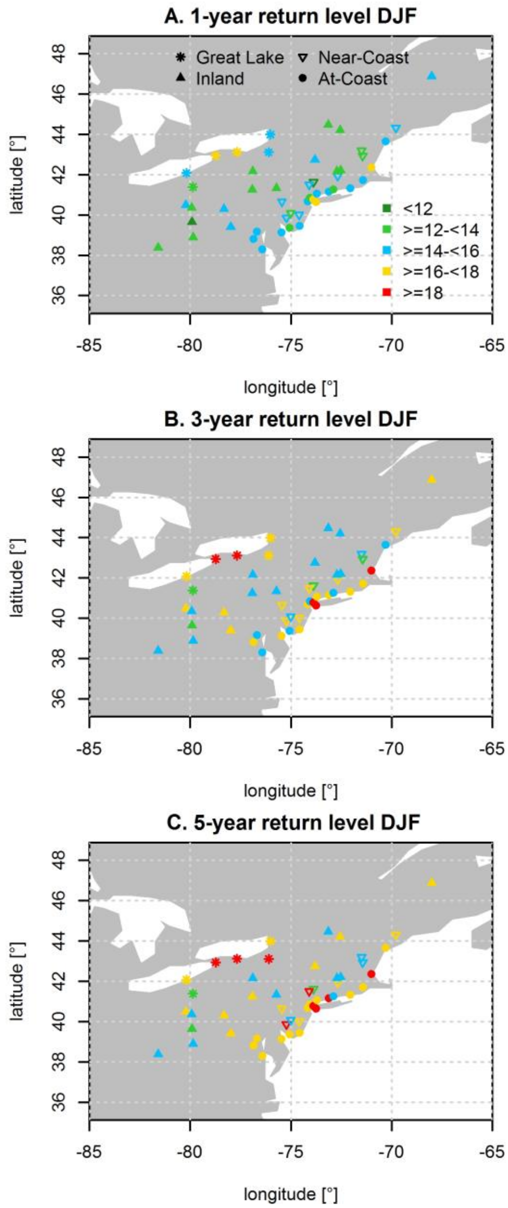

Figure 9: (a) 1-year MAX return level on site basis; (b)-(c) as (a) but for 3-year and 5-year return levels.